Offshore Wind Farm Layout Optimization using Mathematical Programming Techniques

Beatriz Pérez[a], Roberto Mínguez[a], Raúl Guanche[a]

[a] *Environmental Hydraulics Institute "IH-Cantabria"*

Abstract

Offshore wind power is a renewable energy of growing relevance in current electric energy systems, presenting favorable wind conditions in comparison with the sites on land. However, the higher energy yield has to compensate the increment in installation and maintenance costs, thus the importance of optimizing resources. One relevant aspect to increase profitability is the wind farm layout. The aim of this paper is to propose a new method to maximize the expected power production of offshore wind farms by setting the appropriate layout, i.e. minimizing the wake effects. The method uses a sequential procedure for global optimization consisting of two steps: i) an heuristic method to set an initial random layout configuration, and ii) the use of nonlinear mathematical programming techniques for local optimization, which use the random layout as an initial solution. The method takes full advantage of the most up-to-date mathematical programming techniques while performing a global optimization approach, which can be easily parallelized. The performance of the proposed procedure is tested using the German offshore wind farm Alpha Ventus, located in the North Sea, yielding an increment of expected annual power production of 3.52% with respect to the actual configuration. According to current electricity prices in Germany,

this constitutes an expected profit increment of almost 1M€ per year.
Keywords:
Layout optimization, Heuristic optimization, Offshore wind farm, Wake effect

1. Introduction

Wind energy is one of the most profitable renewable energy sources, constituting a proven technology to meet current and future electricity demands. Most of the operating wind farm turbines are on land, however an important part of the future expansion of wind energy, mainly in Europe, is expected to come from offshore sites.

Offshore wind conditions are favorable with respect to sites on land, presenting stronger and steadier wind speeds. However, the advantages with respect to the potential wind resource contrast with the increments of installation and maintenance costs, which must be somehow compensated. This reason has motivated scientist and engineers to focus on optimizing offshore wind farm project designs, focusing on different aspects such as location [1], installation, layout [2, 3, 4, 5], availability, operation and maintenance [6, 7], etc. Note that although all these aspects are relevant, in this study we focus only on the layout optimization.

Once the wind off-shore resource is probabilistically characterized at a particular location, it is possible to strategically position the turbines in order to minimize expected wake effect losses, thus maximizing the expected efficient energy production. This problem is referred to as optimizing the layout of a wind farm. Note that when the wind goes though any turbine, a wake effect is induced downstream decreasing wind speed and increasing wind turbulence. This produces a reduction of energy production in all turbine located within the area of influence of the wake.

Different studies on layout optimization have been proposed in the literature. The first work that addresses this problem is [2], which use genetic algorithms to determine the positions of wind turbines that provide the maximum energy extraction with the minimum installation costs. A decade later, [3] propose the use of an heuristic methodology based on Greedy in order to maximize profits rather than the energy produced in the wind farm. [8] formulates the generalized vertex parking problem (GVP) and obtain the maximum energy production subject to several constraints. However, the author does not clearly state which wake model is used for the study. [9] proposes a multi-objective optimization problem using genetic algorithms, maximizing the energy production and minimizing the failure of the limitations. [5] develops within the auspicious of the Offshore Wind Farm Optimization (OWFLO) project, a more comprehensive study combining an energy production model (taking into account wake effects, electrical losses and turbine availability) with offshore wind farm component cost models. This project aims to pinpoint the major economic hurdles present for offshore wind farm developers by creating an analysis tool that unifies offshore turbine micrositing criteria with efficient optimization algorithms. Finally, [10] proposes the Unrestricted Wind Farm Layout Optimization (UWFLO) methodology, that addresses critical aspects of optimal wind farm planning. It simultaneously determines the optimum farm layout and the appropriate selection of turbines (in terms of their rotor diameters) that maximizes the net power generation.

To our knowledge, all optimization algorithms proposed for layout optimization are based on heuristic procedures, specially Genetic Algorithms [11]. [12] presents an evolutive algorithm to optimize the wind farm layout onshore. The algorithm's optimization process is based on a global wind farm cost model using the initial investment and the present value of the yearly net cash flow during the entire wind-farm life span. [13] proposes a novel evolutionary algorithm for optimal positioning of wind turbines in wind farms. For this case, a realistic model for the wind farm is considered, which includes orography, shape of the wind farm, simulation of the wind speed and direction, and costs of installation, connection and road construction among wind turbines. [14] introduces an ant colony algorithm for maximizing the expected energy output.

The main idea of these methods is to generate, evaluate, and select possible solutions based on different principles, depending on the type of method, until the algorithm is unable to find a better solution. Basically, these methods focus on finding an acceptable solution in an attempt to capture the global optimum. However, they use simplifying assumptions and do not ensure neither local nor the global optimum, which means that most of the times the solutions obtained do not even hold the Karush-Kuhn-Tucker optimality conditions (see [15, 16]). In particular, and regarding the layout optimization problem, existing approaches discretize the possible locations of turbines over a predefined grid which limits the feasible region of possible locations considerably.

The selection of heuristic instead of mathematical programming techniques for layout optimization has been based on two main assumptions:

1. The computational time of gradient-based mathematical programming methods is prohibitive to solve these kinds of problems.
2. The optimal location problem is non-convex, and gradient-based methods provide local solutions. Thus, depending on the initial solution used to start running these algorithms, the global optimum may be skipped.

The aim of this paper is to drop these assumptions by presenting a combined method, heuristic versus gradient-based, to obtain the best offshore wind farm layout over a pre-specified area. The proposed procedure takes full advantage of the state-of-the-art nonlinear programming solvers. Since the global optimum must lie in a convex subregion, which may be identified by the mathematical programming solvers, we look for the global optimum by restarting heuristically the initial solution used to run gradient-based solvers. The proposed methodology has the following advantages:

1. Current state-of-the-art nonlinear mathematical programming solvers are more reliable, numerically robust, and computationally efficient.
2. Nonlinear mathematical programming solvers allow including alternative constraints easily, or objective functions, which do not alter the flow of the methodology.
3. The heuristic method used to generate initial solutions is capable of searching convex subregions. This allows tackling non-convexities.
4. It is easy to include parallelization features in order to increase computational efficiency and reduce computational costs.

5. The final solution holds the Karush-Kuhn-Tucker optimality conditions.
6. It does not require reducing the feasible solution region by gridding the possible location area.

The rest of the paper is structured as follows. Section 2 justifies the wake model selection. Section 3 and Section 4 present the layout optimization methodology formulating the mathematical statement of the problem and the solution algorithm. In Section 5, the proposed method is applied using the German offshore wind farm, Alpha Ventus, and finally, in Section 6 some relevant conclusions are duly drawn.

2. Wake models

A wake is the downstream region of disturbed flow, usually turbulent, caused by a body moving through a fluid. In the case of wind turbines, the wind forces the blades to rotate, thus generating the mechanical energy which is subsequently converted to electricity. This energy extraction decreases the wind speed and increases turbulence at the rear of the turbine, which reduces the energy production at downwind turbines.

Several studies which carry out extensive comparisons between different wake models (see [17, 18, 19, 20]) allow concluding that there is a high uncertainty in all models performance. However, [17], based on the findings from his work, recommends the N.O. Jensen model be used for the energy predictions in offshore wind farms, as it offers the best balance between positive and negative prediction errors. This is the model selected for this study.

For a location i, located on the downstream wake induced by turbine j, and at a distance d_{ij} projected on the wind direction between turbine j and the point of study i, the wake velocity deficit $D_{v_{ij}}$ is given by the following expression:

$$D_{v_{ij}} = 1 - \frac{v_i}{v_j} = \frac{(1 + \sqrt{1 - C_{t_j}})}{\left(1 + \frac{k \cdot d_{ij}}{R}\right)^2}, \tag{1}$$

where v_i is the velocity at location i within the wake, v_j the wind speed reaching turbine j, C_{t_j} is the thrust coefficient associated with velocity v_j, k is the decay factor, and R is the rotor radius.

The decay factor k describes how the wake breaks down by specifying the growth of the wake width per meter traveled downstream. The determination of k is sensitive to factors including ambient turbulence, turbine induced turbulence and atmospheric stability. In a simplified manner, the calculation is performed through the following equation:

$$k = \frac{A}{\ln\left(\frac{z}{z_0}\right)} = \frac{1}{2\ln\left(\frac{h}{z_0}\right)}, \tag{2}$$

where z is the height of the turbine, A a constant approximately equal to 0.5, and z_0 is the surface roughness. Parameter z_0 is crucial in the decay coefficient. There are numerous recommendations [17, 21, 22] for its selection. Typical values for different kinds of terrains are given [21].

This model was first described by [23] and further developed by [24]. It is used in several commercial softwares, such as, WAsP [21], Garrad Hassan WindFarmer [25], and WindPRO [19].

3. Layout problem definition

This study aims to determine the optimal layout of the wind turbines inside an offshore wind farm in order to reduce the wake effects as much as possible. Since we propose to face this problem using mathematical programming techniques, we start by defining the four basic elements required to state any optimization problem [26, 27]: i) data, ii) problem variables, iii) constraints, and iv) the objective function.

Once the main elements of the problem are described, we explain in detail the combined heuristic versus mathematical programming strategy used to solve it.

3.1. Data

The data constitutes the information which is known and required to set and appropriately calculate the objective function and constraints. For this particular case, it can be classified in the following sets:

Wind data. This set includes all wind-related parameters associated with the location:

1. Wind data at 10 meters height in the study area (v_{10}), including both wind speed and directional information. This data is critical to correctly predict on the energy production and evaluate wake losses. It can be based on i) instrumental measurements in the field, which usually provide accurate information although of short length, ii) reanalysis data, which constitutes an alternative to providing long records [28], or iii) a combination of both, i.e. reanalysis data calibrated using instrumental information from satellite or from the field [1].

2. Coefficient of roughness length or surface roughness (z_0), which is required to evaluate the wind speed at different heights.

Turbine data. This set includes all parameters related to the specific turbine:

1. Hub height (z). This information allows us to calculate the required wind speed at the height using an appropriate wind profile.
2. Rotor diameter or radius ($D,\ R$). The energy produced by the turbine is dependent on this value, and also affects the form of the wake.
3. Thrust coefficient (C_t). This information is turbine specific, and is usually given as a curve, which depends on the wind speed at the hub v.
4. Power curve (P_w). This curve defines the energy produced by the turbine as a function of the the wind speed at the hub v. It includes information on the control mechanisms.

Wake effect data. This set includes all parameters required by the wake effect model not previously mentioned:

1. The decay factor k.
2. The minimum distance where the wake model is considered to work appropriately ($d_{\min}$).
3. Number of sectors n_s considered for the energy production calculations.

Wind farm data. This set includes all parameters associated with the wind data:

1. Area where turbines can be located.
2. Number of turbines (N_T) to be allocated within the wind farm area.

3.2. Problem variables

The variables constitute the decisions to be made, which for this particular case are the exact location coordinates of each turbine (x_i, y_i); $\forall i = 1, \ldots, N_T$. These variables are integrated into the variable decision vector $\boldsymbol{x} \in \Re_{N_t \times 2}$ as follows:

$$\boldsymbol{x} = \begin{bmatrix} x_1 & y_1 \\ x_2 & y_2 \\ \vdots & \vdots \\ x_{N_T} & y_{N_T} \end{bmatrix}. \qquad (3)$$

Note that besides wake effects, the appropriate layout of any wind farm is influenced by additional factors, such as, water depth (foundation costs). Water depth could be included into the decision variable vector as an additional coordinate (z_i; $\forall i = 1, \ldots, N_T$). Its consideration would require to define the bathymetry over the wind farm area as data. Nevertheless, this is out of the scope of the paper, and constitutes a subject for further research

3.3. Constraints

The set of constraints determine which decisions are admissible, i.e. define the feasible region of the problem variables. In this paper we have considered two types of constraints:

Minimum distance. The wake model selected ([23]) is known to provide appropriate results for distances higher than four rotor diameters, and for safety reasons, the minimum distance between turbines within the wind farm is limited to four rotor diameters ($d_{min} = 4D$). This restriction can be mathematically expressed as follows:

$$\frac{(x_i - x_j)^2 + (y_i - y_j)^2}{(4D)^2} \geq 1;\ \forall i = 1, \ldots, (N_T - 1);\ \forall j > i. \tag{4}$$

Note that the manner in which constraint (4) is defined facilitates gradient-based methods to converge because of an adequate scaling, i.e. the variable units do not affect the solution.

Wind farm area limits. Turbines must be allocated to a predefined area given as data. The optimization process must ensure that turbines are within the required area. In this paper, we define this limiting area using 4 nodes (quadrilateral). Given these four coordinates $(x_i^L, y_i^L);\ i = 1, 2, 3, 4$ as data, the constraint that ensures turbines remain inside this quadrilateral region is as follows:

$$\begin{vmatrix} x_i & y_i & 1 \\ x_j^L & y_j^L & 1 \\ x_k^L & y_k^L & 1 \end{vmatrix} \geq 0; \begin{cases} \forall i;\ j = 1;\ k = 2 \\ \forall i;\ j = 2;\ k = 3 \\ \forall i;\ j = 3;\ k = 4 \\ \forall i;\ j = 4;\ k = 1. \end{cases} \tag{5}$$

Constraint (5) requires that the area of the four triangles formed by each node-turbine with each pair of consecutive boundary nodes (measured in counterclockwise direction) is always greater than zero.

It was mentioned before that besides wake effects, the appropriate layout of any wind farm is influenced by additional factors. Some of these additional aspects are visual impact, environmental factors, tourism and legal approval, among many others. We assume that the selection of the location limiting area takes into account all these factors.

Note that both restrictions (4) and (5) are non-linear and linear inequality constraints, respectively.

3.4. Objective function: Annual Energy Production (AEP)

Finally, a function that allows us to characterize how good or bad any decision is, must be defined. For this particular case, we have decided to use the expected Annual Energy Production (AEP), which takes into consideration the wake effects and allows quantifying the benefits in terms of profit from the location strategy.

The wake effect depends on wind speed magnitudes and directions. For this reason the calculation of the expected AEP requires the definition of the wind speed probability density function conditional on the direction. Assuming that the conditional distribution is Weibull, which is widely accepted for wind data, the probability density function is defined as follows:

$$f_{V|\theta}(v) = \frac{\delta(\theta)}{\lambda(\theta)}\left(\frac{v}{\lambda(\theta)}\right)^{\delta(\theta)-1} e^{-\left(\frac{v}{\lambda(\theta)}\right)^{\delta(\theta)}}, \tag{6}$$

where v represents the wind speed at the hub height, δ and λ are the shape and scale parameters of the Weibull distribution, respectively, and θ is the wind direction.

The parameters of the distribution (6) need to be estimated from real data, which in our case consist of hourly time series of wind speeds and directions. To facilitate calculations and speed up the objective function evaluation for a given layout configuration, we divide the possible directions into a number of sectors n_s. Data from each sector is fitted to a Weibull distribution. The selection of the number of sectors is very important. A small number is favorable for the Weibull fitting because it increases the length of data records within sectors, but the errors from the wake effect increase because the mean direction is used as the representative for each sector. On the other hand, increasing the number of sectors decreases the quality fit, however it also decreases the wake effect errors. Numerical tests performed with different number of sectors [29] allows us to conclude that the selection of 12 sectors of 30° width provides the best compromise in terms of i) Weibull fitting quality, ii) wake effect errors, and iii) computational time, bounding the errors with respect to the expected AEP below 0.5%. This result is in accordance with conclusions given in [17]. It is important to highlight that increasing the number of sectors, for example, using 360, does not necessarily decrease the error with respect the 12 sectors selection, due to the the fact that Weibull fitting is usually worse for small sectors, and besides, computational times increase considerably. For instance, for the Alpha Ventus case with 12 turbines and a regular grid (defined in section 5), the computational time to evaluate the AEP considering the wake effect changes from about $\approx$ 4 seconds for 12 sectors to $\approx$ 57 seconds for 360 sectors, whereas the errors change from 0.49% to 0.79%. Note that errors have been obtained using, as reference value, the energy calculations for $20 \times 365.25 \times 24 = 175320$ hourly records of wind velocity and direction.

Although the selection of 12 sectors may be an adequate value for practical problems, it is highly recommended to make a previous analysis of the number of sectors required to counter-balance errors and computational performance. For that reason n_s is considered a parameter to be defined by the user.

Once the number of sectors n_s is defined, the expected Annual Energy

Production (AEP) is calculated as follows:

$$\mathrm{AEP} = 8760 \sum_{s=1}^{n_s} \rho_s \sum_{i=1}^{N_T} \left[\int_{v_{c_i}}^{v_{c_o}} f_{V|\theta_s}(v) P_w(v_i)\, dv \right], \tag{7}$$

where 8760 is the mean number of hours per year, ρ_s is the probability of the wind to be within sector s, v_{c_i} and v_{c_o} are, respectively, the cut-in and cut-out velocities defined in the turbine power curve, and $P_w(v_i)$ is the power produced by turbine i for its corresponding wind speed. Note that v_i comes from the perturbed wind speed v at the hub height decreased by the wake effect. These effects depend on the wind direction and the positioning of each turbine compared to the others. The objective function calculation is based on the sum of the energy yield by each turbine for each sector, as shown in equation (7).

The calculation of the expected AEP according to (7) is a key step for the correct performance of the proposed optimization method. To facilitate the understanding of the process the most relevant steps within the algorithm are described below for a given directional sector s:

Wind farm reorientation and renumbering. This step consists of a base change to rotate the cartesian axis by an angle θ measured from the north to the average direction of the study. The rotation can be expressed mathematically as:

$$\boldsymbol{x}' = \left(\begin{bmatrix} \cos\theta_s & -\sin\theta_s \\ \sin\theta_s & \cos\theta_s \end{bmatrix} \boldsymbol{x}^T \right)^T. \tag{8}$$

Once the new coordinates are calculated, it is very simple to renumber turbines ranked according to their vertical coordinate y' in descending order (see Figure 1).

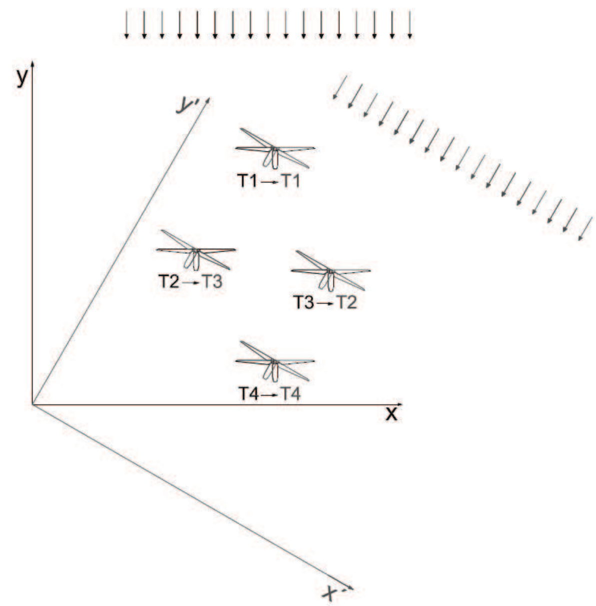

Figure 1: Renumbering of the turbines after the base change.

Note that this step allows us to rapidly select the possible turbine set Ω_i affecting each turbine i due to wake effect, that is, those with cardinality lower than i, i.e. $\Omega_i = \{1, 2, \ldots, i-1\}$.

Velocity evaluation due to the wake effect. For each turbine, the true velocity at the rotor, which may decrease due to the wake effect, is calculated. Given a specific unperturbed velocity v and turbine i, this process entails the following steps which must be repeated with all turbines belonging to set Ω_i:

- **Step 1: Cross sectional area intersection.** Before evaluating the wind speed deficit, one must calculate the area of the wake produced by turbine j that intersects with the rotor swept area of the downstream turbine i, i.e. A_{ij}. This is a geometric problem in which there are four possible cases as shown in Figure 2.

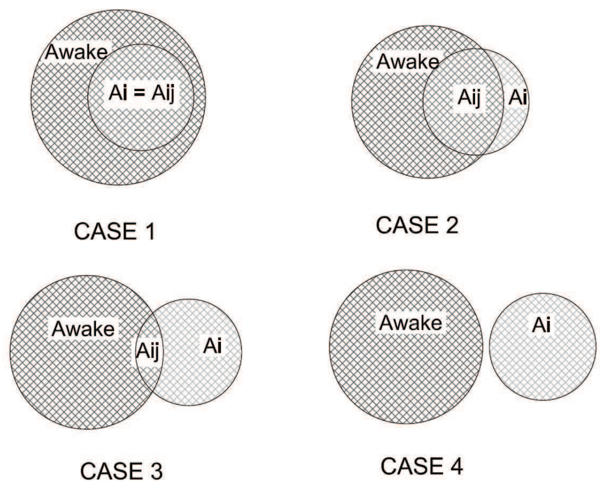

Figure 2: Different possibilities for cross sectional intersection area problem.

- **Step 2: Deficit velocity evaluation.** Once the intersection area A_{ij} is available, the deficit of wind velocity due to the wake effect is calculated according to [21] as follows:

$$D_{v_{ij}} = \frac{(1 + \sqrt{1 - C_{t_j}})}{\left(1 + \frac{k \cdot d_{ij}}{R}\right)^2} \cdot \frac{A_{ij}}{A_i}, \tag{9}$$

where A_i is the rotor area, and the thrust coefficient C_{t_j} is calculated using the curve for the velocity at turbine j, which was previously obtained. Thus the importance in calculating the velocities from upstream to downstream. Note that (9) is a slight modification of expression (1) that takes into account the extent to which the turbine i is affected by the wake of the turbine j.

At this step of the process, we have calculated all deficits $D_{v_{ij}}$; $\forall i \in \Omega_i$ affecting turbine i velocity. [24] proposed an energy balance to calculate the cumulative deficit produced by several turbine wakes, so that the total speed deficit for turbine i is computed as follows:

$$(D_{v_i})^2 = \sum_{\forall j \in \Omega_i} (D_{v_{ij}})^2. \tag{10}$$

According to (1), the unperturbed wind speed at the hub height v due to the wind farm wake effect for turbine i turns into:

$$v_i = v(1 - D_{v_i}). \tag{11}$$

Power output evaluation. The power produced by turbine i is obtained from the given power curve as a function of the calculated wind speed v_i.

Note that the previous steps were explained only for a given i) directional sector, ii) turbine i, and iii) unperturbed velocity v. However, this process is embedded in an integral over the range of possible wind speeds, which is numerically evaluated using the trapezoidal quadrature formula. Numerical tests performed using different quadrature (Simpson) methods and size steps show that the trapezoidal rule using a step size $\Delta v = 0.1$ m/s provides the best counter-balance between small errors (below 0.01%) and computational efficiency (see [29]).

From a mathematical point of view, it would be very easy to include additional factors on the objective function to account for the water depth (foundation costs) or electrical connection to the grid (cable costs). However, this is out of the scope of the paper.

4. Layout optimization

Once the four elements of the optimization problem are defined. The mathematical programming definition is stated as follows:

$$\underset{\boldsymbol{x}}{\text{Maximize}} \quad AEP, \tag{12}$$

given by (7) and subject to constraints (4) and (5).

According to the type of objective function and constraints, this problem is a nonlinear mathematical programming problem with linear and non-linear inequality constraints. It can be efficiently solved using any of the available solvers for nonlinear programming subject to constraints, for instance, solver MINOS [30] or CONOPT [31] under GAMS [32], the Trust Region Reflective Algorithm under Matlab [33, 34], also capable of dealing with nonlinear equality constraints and upper and lower bounds through the function `fmincon`, or interior-point barrier and active set techniques implemented on function `ktrlink` [35], where each algorithm addresses the full range of nonlinear optimization problems, and each is constructed for maximal large-scale efficiency.

Numerical tests performed using functions `fmincon` and `ktrlink` show that these algorithms are capable of finding solutions holding the KKT optimality conditions in a reasonable computational time. However, the problem is that they are suited for finding local minima, and depending on the initial layout configuration used to run the algorithms, different local minima could be found. To overcome this difficulty, we propose a combined method based on two basic steps:

Heuristic initial solution: In an attempt to identify all possible convex subregions, an initial stochastic solution $\boldsymbol{x}^s$ holding constraints (4) and (5) is generated.

Local minima search: Run any mathematical programming technique using the sample solution $\boldsymbol{x}^s$ as a starting value.

Repeating this process allows us to explore all possible local solutions. Although a finite number of iterations does not guarantee that the global optimum is achieved, the probability of succeeding increases with the number of times the proposed sequential procedure is performed. The main idea is to make as many repetitions as possible depending on different factors, such as the time available to carry out the analysis, computational resources, number of turbines. Nevertheless, we will always obtain a good solution, and several rules of thumb may be used to decide reasonable stopping criteria. For example, we could stop the process if we do not improve the best solution obtained so far during a pre-specified number of iterations.

Note that the structure of the problem would allow us to parallelize the process easily, each core may repeat this heuristic-local search process independently. The only requirement is to share the best solution found between cores.

4.1. Heuristic initial solution

The first step of the proposed procedure consists of the simulation of an initial solution, which is used as starting point to run gradient-based algorithms. The aim of this stage is to cover all possible local solutions and facilitate gradient-based algorithm performances. For these reasons, the heuristic generation must fulfill the following conditions:

1. **Condition 1:** The initial solution must cover all possibilities, thus the initial location must be random, being able to locate turbines anywhere within the wind farm area.
2. **Condition 2:** The initial solution must hold the non-linear inequality constraints (4) and linear inequality constraints (5). Note that using initial solutions within the feasibility region speeds up computational performance. However, this step is not customary, as we shall explain later, because mathematical programming techniques include methods to move to the feasible region.
3. **Condition 3:** If there were no constraints on the wind farm location area, the best known solution to avoid wake effects to locate turbines as far away from each other as possible. Thus, we try to cover all study area as much as possible.

In order to fulfill these requirements, we use a two step procedure. The method aims to maximize the use of the area assigned by random spread of the turbines, taking into account constraints (4) and (5):

Uniformly random simulation Simulate N_T uniformly distributed random numbers $\xi_i \sim U(-1,1)$ and $\eta_i \sim U(-1,1)$; $\forall i = 1,\ldots,N_T$.

Note that the probability of locating the coordinate (ξ_i, η_i) in any point within the rectangle is the same.

Rectangle transformation Transform those points from the regular rectangle into the wind farm area defined by points (x_i^L, y_i^L); $i = 1, 2, 3, 4$ as follows:

$$\begin{aligned} x_{i,0}^s &= \sum_{l=1}^{4} N_l(\xi_i, \eta_i) x_l^L; \ \forall i = 1, \ldots, N_T \\ y_{i,0}^s &= \sum_{l=1}^{4} N_l(\xi_i, \eta_i) x_l^L; \ \forall i = 1, \ldots, N_T, \end{aligned} \tag{13}$$

where functions N_l; $\forall l = 1, 2, 3, 4$ are equal to:

$$N_1(\xi, \eta) = \frac{1}{4}(1 - \xi)(1 - \eta) \tag{14}$$

$$N_2(\xi, \eta) = \frac{1}{4}(1 + \xi)(1 - \eta) \tag{15}$$

$$N_3(\xi, \eta) = \frac{1}{4}(1 + \xi)(1 + \eta) \tag{16}$$

$$N_4(\xi, \eta) = \frac{1}{4}(1 - \xi)(1 + \eta). \tag{17}$$

Turbine widespread In order to fully exploit the wind farm area, we try to spread turbines out all over the limiting area. Thus, we perform a triangulation [36] using the simulated points $(x_{i,0}^s, y_{i,0}^s)$; $\forall i = 1, \ldots, N_T$, and then maximize the sum of triangle areas solving the following optimization problem:

$$\underset{(x_i^s, y_i^s);\ \forall i = 1, \ldots, N_T}{\text{maximize}} \quad \sum_{\forall t} A_t \tag{18}$$

subject to (4), (5) and

$$A_t > 0 \,; \forall t, \tag{19}$$

using as starting variables $(x^s_{i,0}, y^s_{i,0});\ \forall i = 1, \ldots, N_T$. A_t is the area of triangle t, which can be calculated using the determinant formula:

$$A_t = \frac{1}{2} \begin{vmatrix} x_{t_1} & y_{t_1} & 1 \\ x_{t_2} & y_{t_2} & 1 \\ x_{t_3} & y_{t_3} & 1 \end{vmatrix} \,; \forall t. \tag{20}$$

Constraint (19) avoids triangle overlapping and edge crossing when they are distorted by moving their vertices. The optimal solution $(x^s_i, y^s_i);\ \forall i = 1, \ldots, N_T$ of this problem hold constraints (4) and (5), and is known in advance, since the maximum sum of areas must be equal to the wind farm limiting area, as shown in Figure 3. This problem is a nonlinear mathematical programming problem easily solvable using any of the previously mentioned algorithms.

The initial solution $\boldsymbol{x}^s = (x^s_i, y^s_i);\ \forall i = 1, \ldots, N_T$ holds the three required conditions and is used as the starting point to run the gradient-based algorithm.

Note that even though the use of this method may seems like killing ants with a sledgehammer, it has the following advantages:

1. Constraints (19) increase computational performance, since the feasible region is reduced. Once the optimal solution is obtained, we could change turbine positions within the same locations and the AEP remains the same. Besides, these constrains are also used within the

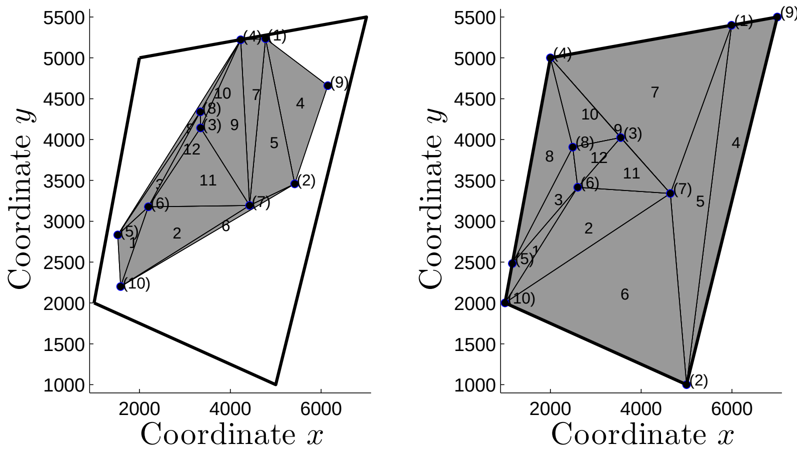

Figure 3: Initial and final location used as starting point, including the selected triangulation.

AEP optimization procedure.

2. Regarding computational performance, the executing time to solve this problem is negligible in comparison with the AEP optimization procedure.

Nevertheless, alternative methods holding conditions 1 and 3 could be used instead, such as: i) locating four turbines in the corners, ii) randomly positioning of the rest of turbines within the wind farm area, and iii) using this configuration as starting point for the nonlinear optimization procedure. Condition 3 would hold at the final optimum after running the optimization routine. In fact, different procedures for selecting the initial location of turbines could be used instead provided that i) it distributes turbines all over the area and ii) allows obtaining different local solutions during the execution of the method.

4.2. Local minima search

Once the initial solution from the heuristic procedure is obtained, the nonlinear mathematical programming algorithm is executed.

Note that from a practical point of view, and according to results obtained from numerical tests using different algorithms, we decided to slightly change the local maxima search strategy. Thus, we use function `ktrlink` within Matlab, repeating the combined process a fixed number of times M. Once the best solution from the M iterations is achieved, this is the candidate to be the global solution. Then we run solver `fmincon` to slightly improve results.

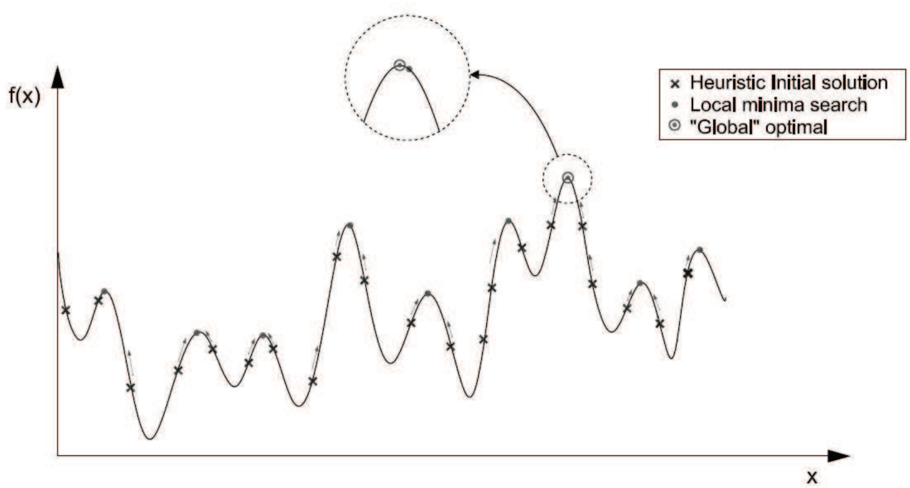

Figure 4: Graphical interpretation of the combined heuristic-gradient base layout optimization strategy.

The reason for this selection is graphically explained in Figure 4. We initially use function `ktrlink` because it obtains a local maximum faster than `fmincon`. However, once the "global" optimal $\boldsymbol{x}_0^*$ is achieved, function `fmincon` slightly improves the objective function providing the final "global " optimal solution $\boldsymbol{x}^*$. Figure 4 shows i) the starting points used to look for convex subregions, ii) the local maxima and iii) the global maximum.

Note that although there is no guarantee that $\boldsymbol{x}^*$ is the true global solution, the chances of finding it increase as M increases. However, this methodology, unlike others, guarantees the optimality conditions of the solution. Furthermore, this gradient-based process could be used to refine solutions obtained from other heuristic methods.

5. Case study: Alpha Ventus

To show the functioning and the potential of the proposed methodology, we select as a case study the Alpha Ventus wind farm. It was the first offshore wind farm to be constructed in open sea conditions (North Sea), 60 kilometres away from the coast, in the midst of extreme winds, weather and tides.

Technically, Alpha Ventus [37] is equipped with the most advanced technologies, specifically designed for offshore wind farms. The wind turbines are placed in a grid-like formation with gaps of approximately 800 meters between each turbine, in a rectangle with a total surface area of four square kilometres. The wind farm has two types of turbines: the Multibrid M5000 and the REpower 5M, two of the largest models in the world.

For this application, it is assumed that the wind farm has 12 identical turbines, NREL 5 MW type [38]. The hub height and rotor diameter are $z = 90$ and $D = 126$ meters, respectively. Power curve (v, P_w) is illustrated in Figure 5 (a). It is a sigmoid function including three different regions: i)

$v < v_{c_i} = 3$ m/s, ii) $v_{c_i} \leq v < v_r = 11.3$ m/s and $v_r \leq v < v_{c_o} = 25$ m/s. The thrust curve $(v,\ C_t)$ is shown in Figure 5 (b). Both curves must be provided by the manufacturer.

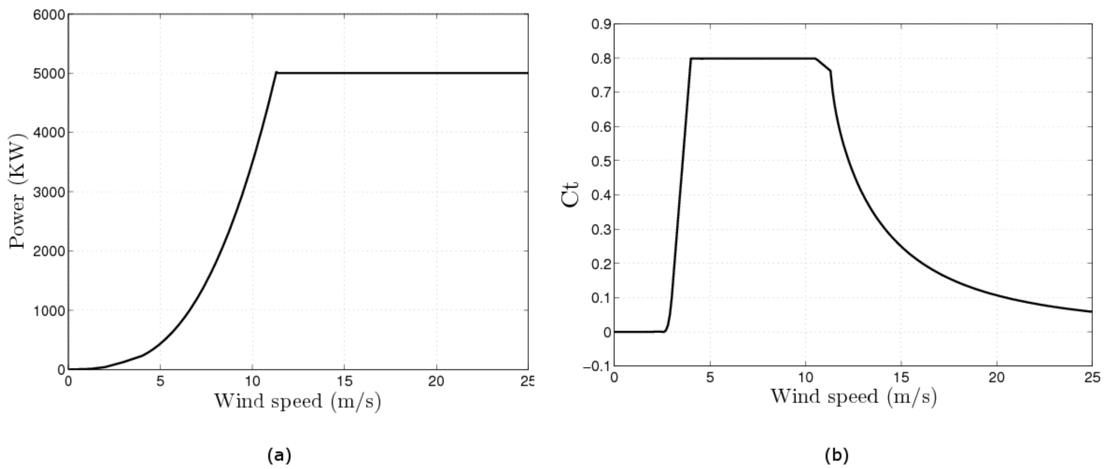

Figure 5: Characteristic curves of 5MW NREL Turbine: a) Power output, and b) Trust coefficient.

Wind data at 10 meters height in the study area is obtained from the SeaWind database [28], which constitutes an hourly wind reanalysis over a 15 km spatial resolution grid for the entire 1989-2009 period, covering the South Atlantic European region and the Mediterranean basin. The logarithmic wind speed profile is chosen to achieve the wind speed at the hub height $z = 90$ meters. The equation of the profile is as follows:

$$v = v_{10}\left(\frac{\ln(Z/z_0)}{\ln(Z_{10}/z_0)}\right) \tag{21}$$

where z_0 is the coefficient of roughness length, which has a value for offshore zones of 0.0002 meters; v and v_{10} are the wind speeds at 90 and 10 meters; Z and Z_{10} are the heights at 90 and 10 meters, respectively. Figure 6 shows the wind rose in the study area.

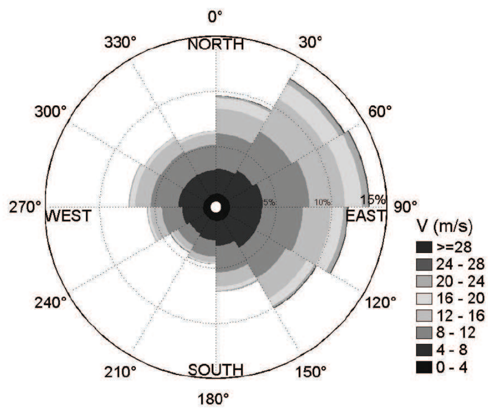

Figure 6: Wind rose for the Alpha Ventus location.

According to the available data, the expected annual AEP considering no wake effect and total availability is equal to 306.9 GWh using 12 sectors, and 308.98 GWh considering the hourly wind speed and direction set during 20 years. Using (7) and considering the wake effect, we obtain the results provided in Table 1 for the actual layout of Alpha Ventus. Results are given by sectors, the percentage of losses due to wake effects for each sector varies from $\approx$ 0% up to $\approx$ 1.5%. The total expected annual AEP is equal to 293.274 GWh, which represents a 4.44% reduction due to wake losses. If we consider the expected annual AEP using the complete data set, the expected annual AEP is equal to 291.364 GWh, which represents a 5.7% reduction due to wake losses. The error of the AEP using 12 sectors is 0.65%. Note that those sectors whose percentage of losses in Table 1 is zero, we expect them to have low values but not null. This result is due to the approximation of the AEP. However, as we shall see, this fact does not invalid results.

Table 1: Annual expected AEP considering wake effects and the actual Alpha Ventus layout.

	Original layout	
	AEP	Wake
Nsector	(GWh annual)	(%)
1	31.429	0.092
2	41.497	1.507
3	46.618	0
4	37.856	0
5	27.424	1.229
6	19.713	0.072
7	10.347	0.047
8	8.471	0.494
9	15.038	0
10	21.703	0
11	16.631	0.931
12	16.545	0.068
Total	293.274	4.440

The proposed methodology is applied to obtain the optimal layout for the 12 turbines on Alpha Ventus. Results are given in Table 2, where we present productions associated with: i) the initial random configuration obtained using the heuristic procedure $\boldsymbol{x}^s$, and ii) the pseudo-global optimum ($\boldsymbol{x}^*$) obtained throughout the gradient base strategy, using $\boldsymbol{x}^s$ as a starting point. According to these results, the following observations are pertinent:

1. The optimal expected annual AEP is equal to 304.809 GWh, reducing the wake effect from 4.44% for the actual layout, to 0.682% at the pseudo-global optimum.
2. If the complete data record is used to calculate the AEP, the optimal expected annual AEP is equal to 302.230 GWh, reducing the wake effect from 5.70% for the actual layout, to 2.18% at the pseudo-global

optimum. This means that the bias is consistent and the method reduces wake effects for both approaches: i) with 12 sectors and ii) using the 20 years data record.

3. The maximum loss due to wake effect is reduced from 1.507% for sector 2 and the actual layout, to 0.194% for sector 6 at the pseudo-global optimum.
4. The initial solution $\boldsymbol{x}^s$ which allows achieving the pseudo-global optimum, does not necessarily constitute a good solution per se. Note that losses due to wake effect for this initial solution are 6.012%, higher than those for the actual configuration.
5. The optimization strategy tends to decrease wake effects for those sector with higher expected AEP. Note that for sectors 3 and 4, the corresponding wake effects are null, and for sector 2, they are close to zero. We remind readers that these results are approximations.
6. The optimization procedure provides an improvement of expected AEP of 3.758% with respect to the actual configuration and using 12 sectors, and 3.52% if we consider the whole data record.

Figure 7 depicts the evolution of wakes for a specific sector (3, 75°NE) and wind speed (15 m/s), i.e. the most likely sector. Note that with the initial simulation, turbines 4, 5, 9, 11 and 12 are under wake effect, however, with the optimal layout, the original flow speed reaches all turbines. Figure 8 shows analogous results to those of Figure 7 in sector 2 (45°NE), for original and optimal layouts. Note the considerable differences between the actual configuration and the optimal.

In economic terms, and assuming a production cost of 0.064 €/KWh

Table 2: Annual expected AEP considering wake effects using the optimization framework proposed in this paper.

	Initial Simulation ($\boldsymbol{x}^s$)		Optimal layout ($\boldsymbol{x}^*$)	
Nsector	AEP_0 (GWh annual)	Wake (%)	AEP_{opt} (GWh annual)	Wake (%)
1	29.682	0.662	31.148	0.184
2	44.522	0.522	46.035	0.029
3	43.366	1.059	46.618	0
4	36.054	0.587	37.856	0
5	29.496	0.554	31.196	0
6	18.641	0.421	19.337	0.194
7	9.534	0.312	10.161	0.107
8	9.447	0.176	9.958	0.010
9	13.519	0.495	15.038	0
10	20.434	0.414	21.703	0
11	18.159	0.433	19.488	0
12	15.595	0.377	16.269	0.158
Total	288.448	6.012	304.809	0.682

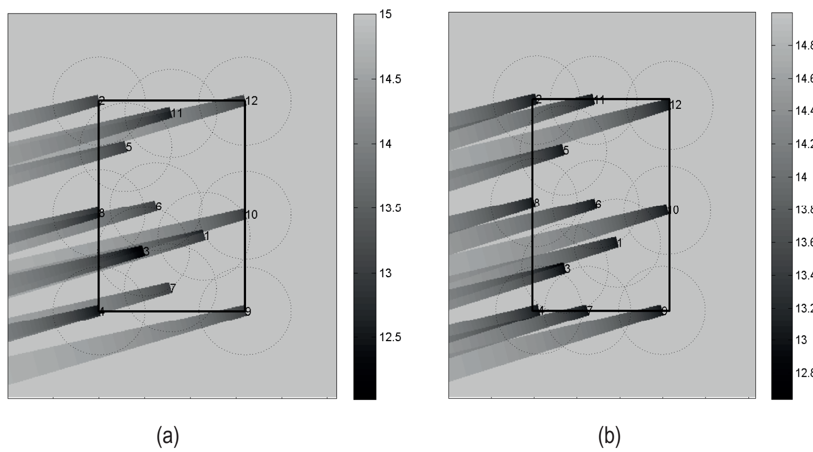

Figure 7: Evolution of the wakes for a 15 m/s wind in sector 3 (75°NE): a) Initial simulation, and b) Optimal layout.

(regardless of the initial investment costs) and a selling price of 0.15 €/KWh, the profit increment due to the reallocation of turbines according to the locations obtained from the proposed procedure, is equal to 0.9921M€ per

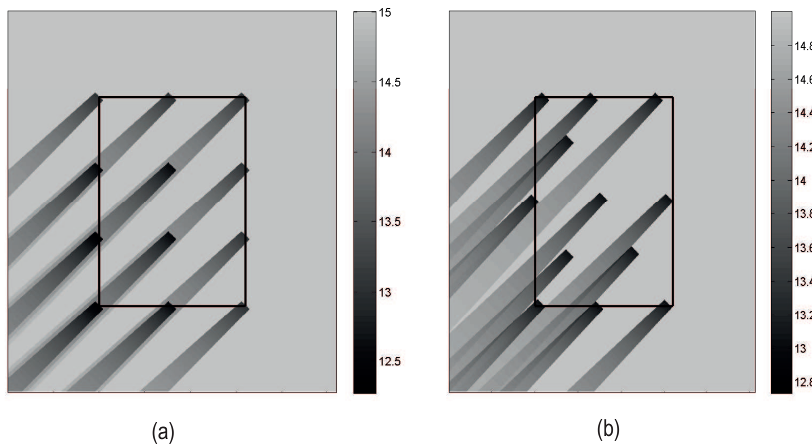

Figure 8: Evolution of the wakes for a 15 m/s wind in sector 2 (45°NE): a) Original layout, and b) Optimal layout.

year using 12 sectors, and 0.9422M€ per year if we consider the whole data record. Both amounts justify the effort performing the layout optimization of any off-shore wind farm.

Finally, and in order to study the sensitivity of the proposed procedure to wind directional data characterization, we have performed new calculations rotating the original wind rose shown in Figure 6 with different angles. Results in Table 3 demonstrate that the optimal layout always provides better performance with respect to the actual configuration based on a regular grid. This result is not surprising since the method tries to accommodate the turbines so that there are no wake conflicts for each directional sector. Since it is impossible to avoid wake effects all over the 360°, the method gives priority to those sectors with higher AEPs, but somehow improves performance throughout the circumference.

Table 3: Sensitivity Analysis with respect to wind directional information for Alpha Ventus case study.

	Original layout		Optimal layout	
Rose	*AEP* (GWh annual)	Wake (%)	*AEP* (GWh annual)	Wake (%)
Rot.0	293.274	4.440	304.809	0.682
Rot. 90	293.017	4.524	304.119	0.906
Rot. 180	293.274	4.440	304.769	0.695
Rot. 270	293.017	4.524	304.216	0.875
Random	143.03	6.589	148.96	2.717

5.1. Efficiency of a Wind Farm: Installed capacity per km^2

So far, the number of turbines to be allocated has been considered as data. However, this could be an additional variable to be optimized. To study how the optimal efficiency within a given area changes with respect to the number of installed turbines, i.e. installed capacity, we have repeated the optimization process using a different number of turbines. Note that the wind farm Alpha Ventus has an actual installed capacity of 15.625 MW/km^2. The efficiency achieved with the optimized layout is 99.25% versus 95.51% obtained with the grid layout.

Figure 9 shows the efficiencies achieved for different numbers of turbines in the two stages of the optimization methodology. It also shows the efficiency achieved with the typical grid layout. Note that if the installed power capacity per km^2 increases, the efficiency is reduced; in other words, the wake effects become more important. In addition, we can also observe that the higher the installed power capacity, the lower the magnitude of improvement we obtain from the optimization algorithm proposed in this paper. This effect is due to the wind farm saturation, which reduces the number of possible turbine locations across the area. Note that with 23 turbines the problem is

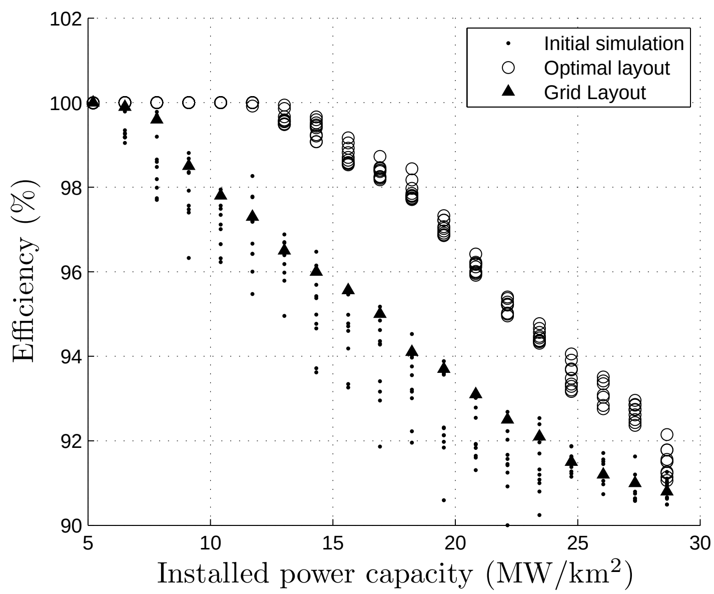

Figure 9: Efficiency vs. installed power capacity per km^2.

unfeasible due to the fact that there are no layouts which satisfy the problem constraints (Minimum distances).

Another important reason is that in the N.O. Jensen wake model, the total velocity deficits inside the wind farm quickly reach an equilibrium level (see [24]) and therefore as the wind farm increases, the layout of the inside turbines start losing importance, as the wake effects inside the wind farm become more homogeneous.

5.2. Saturation area

To analyze the saturation effect, Figure 10 illustrates the saturation of the wind farm. This figure shows box-plots related to: i) the root mean square distances between the turbine locations, with values converging to a constant around 1400 m, and ii) expected annual energy production (AEP), in which the maximum value is 518 GWh for 22 turbines. These box-plots have been generated running 100 cases for each installed capacity (number of turbines).

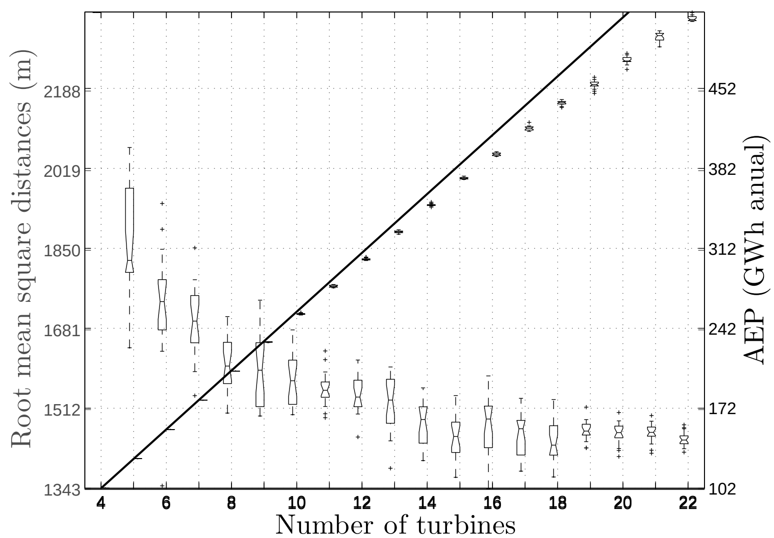

Figure 10: Combined box-plots: AEP and root mean square distances.

The evaluation of the root mean square of distances allows us to study the difference between the optimal layouts, proving that the more saturated the area, the solutions are more similar to each other, resembling the grid layout. According to Figure 10, it is clear that for the study area with 19 or 20 turbines, the adjustment of AEP data ceases to be linear, i.e. the efficiency decreases. If an economic study is carried out, this number of turbines would correspond to the value where the assigned area reaches its maximum profitability, because losses induced by wake effect do not compensate the installation of more turbines. The graph is computed for up to 22 turbines, because there are no possible layouts with 23 turbines satisfying the minimum distance between turbines required.

5.3. Computational time

Finally, the performance of the algorithm under different situations is analyzed by comparing the estimated complexity of the algorithm with the experimental computational running times [1].

In Figure 11 the experimental times obtained during the different test cases are plotted (50 test cases for each installed capacity).

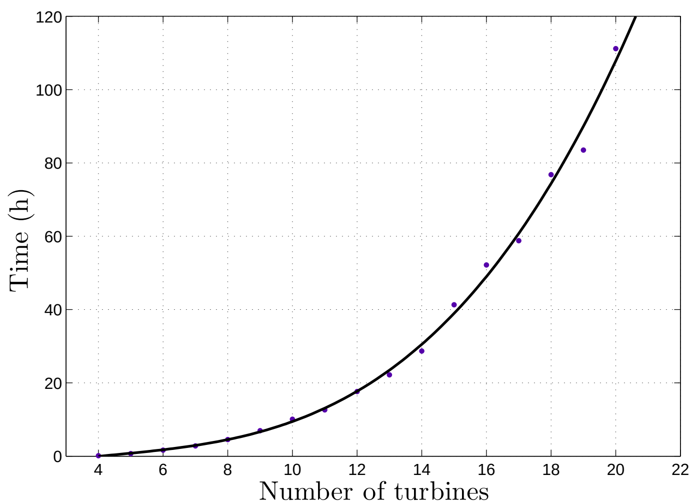

Figure 11: Running time for 50 cases as a function of the number of turbines.

It is important to note that experimental time values were not measured under the exact same conditions. Therefore, Figure 11 should be used solely

[1]Computer characteristic: Intel Core i5-2400 3.10GHz, 3.24GB RAM running under Windows XP Professional

as a reference to know the approximate running time for the simulation with N turbines.

6. Conclusions

This paper proposes a new method to maximize the expected power production of offshore wind farms by setting the appropriate layout, i.e. minimizing the wake effects, and indirectly, reducing the fatigue effects on the turbines, which on turn reduce its service life.

The method uses a sequential procedure for global optimization consisting of two steps: an heuristic method to set an initial random layout configuration, and the use of nonlinear mathematical programming techniques for local optimization, which use the random layout as an initial solution.

The performance of the proposed procedure is tested using the German offshore wind farm Alpha Ventus, yielding an increment of the expected annual power production of 3.758% compared to the actual configuration. A comparison between the installed capacity per km^2 and the efficiency of the wind farm is also carried out to determine the efficiency of the algorithm when the size of the wind farm is increased. It is found that when the wind farm has many turbines and the turbines have little freedom to move within the wind farm area, the effectiveness of the algorithm is reduced and the output layout gives similar results as that of any grid-like layout. On the other hand, for smaller wind farms the improvement in energy production is remarkable and the effectiveness of the program is proven.

The proposed methodology has many advantages: the nonlinear mathematical programming solvers are numerically robust and computationally efficient; they can include alternative constraints or objective functions without altering the flow of the methodology; the heuristic method used to generate initial solutions is capable of searching convex subregions; it is easy to include parallelization features; the final solution holds the Karush-Kuhn-Tucker optimality conditions; and the methodology does not requiere reducing the feasible solutions region by gridding the possible location area.

There is still much work to be done in the field of wind farm optimization. These include wake modeling to properly predict the wind decay (and therefore the power losses). Other physical aspects such as foundations or cabling, human aspects as visual effects and area restrictions, and mathematical topics regarding the optimization approaches must also still be reviewed in detail.

References

[1] A. Espejo, R. Mínguez, A. Tomás, M. Menéndez, J. M. Méndez, I. J. Losada, Directional calibrated wind and wave reanalysis databases using instrumental data for optimal design of offshore wind farms, in: OCEANS 2011–EUROPE, 2011, pp. 1–9. doi:10.1109/Oceans-Spain.2011.6003592.

[2] G. Mosetti, C. Poloni, B. Diviacco, Optimization of wind turbine positioning in large wind farms by means of a genetic algorithm, Journal of Wind Engineering and Industrial Aerodynamics 51 (1) (1994) 105 – 116. doi:10.1016/0167-6105(94)90080-9.

[3] U. Ozturk, B. Norman, Heuristic methods for wind energy conversion

system positioning, Electric Power Systems Research 70 (3) (2004) 179 – 185. doi:10.1016/j.epsr.2003.12.006.

[4] S. A. Grady, M. Y. Hussaini, M. M. Abdullah, Placement of wind turbines using genetic algorithms, Renewable Energy 30 (2) (2005) 259 – 270. doi:10.1016/j.renene.2004.05.007.

[5] C. N. Elkinton, J. F. Manwell, J. G. McGowan, Offshore wind farm layout optimization (OWFLO), Project: Preliminary results, Tech. rep., University of Massachusetts (2006).

[6] L. W. M. M. Rademakers, H. Braam, M. B. Zaaijer, G. J. W. Van Bussel, Assessment and optimization of operation and maintenance of offshore wind turbines, in: Proceedings of the European Wind Energy Conference (EWEC), Madrid, Spain, 2003.

[7] R. Mínguez, M. Martínez, O. F. Castellanos, R. Guanche, Component failure simulation tool for optimal electrical configuration and repair strategy of off-shore wind farms, in: OCEANS, 2011 IEEE - Spain, 2011, pp. 1–10. doi:10.1109/Oceans-Spain.2011.6003599.

[8] S. Donovan, H. D. Sherali, J. C. Smith, Wind farm optimization, Tech. rep., University of Auckland, Engineering science department (2005).

[9] A. Kusiak, Z. Song, Design of wind farm layout for maximum wind energy capture, Renewable Energy 35 (3) (2010) 685–694. doi:10.1016/j.renene.2009.08.019.

[10] S. Chowdhury, J. Zhang, A. Messac, L. Castillo, Unrestricted wind

farm layout optimization (UWFLO): Investigating key factors influencing the maximum power generation, Renewable Energy 38 (2012) 16–30. doi:10.1016/j.renene.2011.06.033.

[11] C. N. Elkinton, J. F. Manwell, J. G. McGowan, Algorithms for offshore wind farm layout optimization, Wind Engineering 32 (1) (2008) 67–84. doi:10.1260/030952408784305877.

[12] J. Serrano, A. G. González, J. Castro, J. Riquelme, M. Burgos, Optimization of wind farm turbines layout using an evolutive algorithm, Renewable Energy 35 (2010) 1671–1681. doi:10.1016/j.renene.2010.01.010.

[13] B. Saavedra-Moreno, S. Salcedo-Sanz, A. Paniagua-Tineo, A. Portilla-Figueras, Seeding evolutionary algorithms with heuristics for optimal wind turbines positioning in wind farms, Renewable Energy 36 (2011) 2338–2844. doi:10.1016/j.renene.2011.04.018.

[14] Y. Eroğlu, Y. Ulusam, Design of wind farm layout using ant colony algorithm, Renewable Energy 44 (2012) 53–62. doi:10.1016/j.renene.2011.12.013.

[15] G. N. Vanderplaats, Numerical Optimization Techniques for Engineering Design, McGraw-Hill, New York, 1984.

[16] M. S. Bazaraa, H. D. Sherali, C. M. Shetty, Nonlinear Programming. Theory and Algorithms, 2nd Edition, John Wiley & Sons, New York, 1993.

[17] D. R. Vanluvanee, Investigation of observed and modelled wake effects at horns rev using windpro, Report, Technical University of Denmark, MEK Department, Fluid Mechanics Section, Denmark (2006).

[18] T. Sorensen, M. L. Thogersen, P. Nielsen, Adapting and calibration of existing wake models to meet the conditions inside offshore wind farms, Report, EMD International A/S, Denmark (2008).

[19] Windpro, EMD International A/S (2011).
URL `http://www.emd.dk/`

[20] J. R. Douwe, Validation of wind turbine wake models. using wind farm data and wind tunnel measurements, Master's thesis, Delft University of Technology. Faculty of Aerospace Engineering, Netherlands (2007).

[21] Wasp wind atlas analysis and application program, Risø National Laboratory. Wind Energy Department (2011).
URL `http://www.wasp.dk/`

[22] M. L. Thogersen, Wind turbine wake modelling and wake generated turbulence, Report, EMD International A/S, Denmark (2011).

[23] N. O. Jensen, A note on wind generator interaction, Report, Ris National Laboratory, Roskilde, Denmark (1984).

[24] I. Katic, J. Hostrucp, N. O. Jensen, A simple model for cluster efficiecy, European wind energy association conference and exhibition, Rome, 1986.

[25] G. Hassan, P. Ltd., GH WindFarmer Theory Manual (2004).

[26] E. Castillo, A. J. Conejo, P. Pedregal, R. García, N. Alguacil, Building and Solving Mathematical Programming Models in Engineering and Science, John Wiley & Sons Inc., New York, 2001, pure and Applied Mathematics: A Wiley-Interscience Series of Texts, Monographs and Tracts.

[27] A. J. Conejo, E. Castillo, R. Mínguez, R. García-Bertrand, Decomposition techniques in mathematical programming. Engineering and science applications, Springer-Verlag Berlin Heidelberg, New York, 2006.

[28] M. Menéndez, A. Tomás, P. Camus, M. García-Díez, L. Fita, J. Fernández, F. J. Méndez, I. J. Losada, A methodology to evaluate regional-scale offshore wind energy resources, in: OCEANS, 2011 IEEE - Spain, 2011, pp. 1–8. doi:10.1109/Oceans-Spain.2011.6003595.

[29] B. Pérez, Estrategia de optimización del layout de parques eólicos offshore, Master's thesis, Environmental Hydraulics Institute, Cantabria University, Santander (2012).

[30] B. A. Murtagh, M. A. Saunders, MINOS 5.5 Users Guide, Report SOL 83-20R SOL 83-20R, Department of Operations Research, Stanford University, Stanford, California (1998).

[31] A. Drud, CONOPT: A system for large scale nonlinear optimization, Reference manual for CONOPT subroutine library, ARKI Consulting and Development A/S, Bagsvaerd, Denmark (1996).

[32] A. Brooke, D. Kendrick, A. Meeraus, R. Raman, GAMS: A user's guide, GAMS Development Corporation, Washington, 1998.

[33] T. F. Coleman, Y. Li, On the convergence of reflective newton methods for large-scale nonlinear minimization subject to bounds, Mathematical Programming 67 (2) (1994) 189–224.

[34] T. F. Coleman, Y. Li, An interior, trust region approach for nonlinear minimization subject to bounds, SIAM Journal on Optimization 6 (1996) 418–445.

[35] R. H. Byrd, J. Nocedal, R. A. Waltz, KNITRO: An integrated package for nonlinear optimization, in: G. di Pillo, M. Roma (Eds.), Large-Scale Nonlinear Optimization, 2006, pp. 35–59.

[36] C. B. Barber, D. P. Dobkin, H. T. Huhdanpaa, The quickhull algorithm for convex hulls, ACM Transactions on Mathematical Software 22 (4) (1996) 469–483.

[37] Alpha ventus (2011).
URL `http://www.alpha-ventus.de,`

[38] J. Jonkman, S. Butterfield, W. Musial, G. Scott, Definition of a 5-MW reference wind turbine for offshore system development, Report, National Renewable Energy Laboratory (2009).